Quantitative analysis of lymphocyte exhaustion markers in patients with localized clear cell renal cell carcinoma

RAQUEL GONZÁLEZ-GARZA[1], ADRIÁN GUTIÉRREZ-GONZÁLEZ[2], NALLELY LÓPEZ-LÓPEZ[1], RAQUEL GARZA-GUAJARDO[3], JUAN PABLO FLORES-GUTIÉRREZ[3], MARIO CÉSAR SALINAS-CARMONA[1], VÍCTOR MANUEL OYERVIDES-JUÁREZ[4], MARCO ALBERTO OCAÑA-MUNGUÍA[2], JOSÉ HÉCTOR ELIZONDO-JASSO[3] and MANUEL MEJÍA-TORRES[1]

[1]Service of Immunology, University Hospital 'José Eleuterio González', Autonomous University of Nuevo León, Monterrey, Nuevo León 64460, Mexico; [2]Service of Urology, University Hospital 'José Eleuterio González,' Autonomous University of Nuevo León, Monterrey, Nuevo León 64460, Mexico; [3]Service of Pathology, University Hospital 'José Eleuterio González', Autonomous University of Nuevo León, Monterrey, Nuevo León 64460, Mexico; [4]Service of Oncology, University Hospital 'José Eleuterio González', Autonomous University of Nuevo León, Monterrey, Nuevo León 64460, Mexico

Received February 14, 2025; Accepted July 14, 2025

DOI: 10.3892/ol.2025.15245

Abstract. Clear cell renal cell carcinoma (ccRCC) is a neoplastic disease associated with poor prognosis. Localized disease is successfully treated with nephrectomy; however, advanced disease often requires the combined use of immunotherapy and targeted therapy. To the best of our knowledge, there is no validated method to predict immunotherapy response and there is a lack of knowledge regarding the expression kinetics of exhaustion receptors in the early stages of ccRCC. In the present study, immunohistochemistry and flow cytometry were performed to evaluate the expression levels of five biomarkers associated with immune dysfunction [programmed cell death protein-1 (PD-1), lymphocyte activation gene 3 (LAG-3), T-cell immunoglobulin and mucin domain containing-3 (TIM-3), cytotoxic T lymphocyte-associated protein-4 (CTLA-4) and programmed death ligand-1 (PD-L1)] in 20 patients diagnosed with localized ccRCC. Immunohistochemistry demonstrated that ccRCC tissue was highly positive for CD3, with low expression of PD-L1 and CTLA-4. Based on flow cytometry, the infiltrating leukocytes were mostly $CD8^+$ lymphocytes and monocytes. In tumors, decreased expression levels of LAG-3, TIM-3, CTLA-4 and PD-L1 were reported; however, expression levels of PD-1 remained unchanged. Sample stratification according to the nuclear grade demonstrated no changes in the evaluated markers. Finally, the 12-month follow-up of blood biomarkers revealed no change in the receptors, except for CTLA-4. The results of the present study suggested that immune exhaustion, defined as increased expression of exhaustion receptors in lymphocytes, was not present in tissues from patients with ccRCC with localized disease.

Correspondence to: Dr Manuel Mejía-Torres, Service of Immunology, University Hospital 'José Eleuterio González', Autonomous University of Nuevo León, 235 North Gonzalitos Avenue, Monterrey, Nuevo León 64460, Mexico
E-mail: mmejia.me0126@uanl.edu.mx

Key words: localized clear cell renal cell carcinoma, exhausted lymphocytes, predictive biomarkers, tumor-immune microenvironment, flow cytometry, immunopathology

Introduction

Renal cell carcinoma (RCC) is an aggressive neoplastic disease of the renal parenchyma that accounts for 2-3% of all diagnosed cancer types (1,2). Among these subtypes, clear-cell RCC (ccRCC) is the most frequent and is characterized by intrinsic chemoresistance (3,4). Overall, ccRCC is diagnosed late in up to 50% of patients, with a median survival of 6-10 months (5,6).

In cancer, lymphocytes develop a hypofunctional state known as immune exhaustion, in which cells exhibit increased expression of immune checkpoints or exhaustion receptors. Immunotherapy reverses this state of exhaustion by blocking the interaction between checkpoints and their ligands, leading to the activation of antitumor immunity (7,8). The approved therapies for advanced RCC include tyrosine kinase inhibitors (targeted therapy) and immune checkpoint inhibitors (ICIs). Currently, there are five ICIs approved for the treatment of advanced RCC: i) Nivolumab and pembrolizumab, which target programmed cell death protein-1 (PD-1) expressed on lymphocytes; ii) ipilimumab, which targets cytotoxic T lymphocyte-associated protein-4 (CTLA-4) also expressed on lymphocytes; and iii) atezolizumab or avelumab, which target the programmed death ligand-1 (PD-L1) on cancer and stromal cells (9-12). In cancer, the upregulation of ligands such as PD-L1 on stroma and tumor cells have immunosuppressive effects on lymphocytes via ligation of the inhibitory receptors CTLA-4 and PD-1. The use of ICIs block these inhibitory signals, which restores the cytotoxic function of infiltrating lymphocytes (7). However, the lack of consensus

on predictive tools for guiding the use of ICIs prevents their widespread applicability, which is a notable issue considering the cost-effectiveness and side effects associated with these therapies (13,14).

Since localized disease can be successfully treated with surgery, there is a lack of studies analyzing the expression of markers such as PD-1, CTLA-4 and PD-L1 during the early stages of the disease. To address this knowledge gap, the present study aimed to evaluate the expression levels of ICI targets [PD-1, PD-L1, CTLA-4, lymphocyte activation gene 3 (LAG-3) and T-cell immunoglobulin and mucin domain containing-3 (TIM-3)] in blood and tumors obtained from a small cohort of patients diagnosed with localized ccRCC. The expression levels of these markers across three tissues were compared: Blood and tumor tissue from patients with ccRCC, and blood from a group of healthy controls. Furthermore, the expression levels of the markers associated with the nuclear grade in tumors and changes in blood after a short-term follow-up of 12 months were evaluated.

Materials and methods

Patient recruitment. The present study included 20 patients diagnosed with ccRCC who underwent elective localized nephrectomy (median age, 62 years; range, 44-71 years) and 10 control subjects (median age, 62 years; range, 55-72 years) who were considered healthy based on medical history and did not have any prior diagnosis of cancer, chronic inflammatory diseases, autoimmune disorders or current infections. Patients and controls were recruited from the Service of Urology at the University Hospital 'Dr José Eleuterio González' (Nuevo León, Mexico) between January 2022 and January 2024 (Table I). Patients were excluded if they were diagnosed with metastatic disease or RCC variants other than ccRCC. The present study was approved by the Institutional Ethics Committee (approval no. IN23-00002) and all participants provided written informed consent before enrollment. Peripheral venous blood samples (4 ml) were obtained on the day before the scheduled nephrectomy (n=20) and after 12 months of clinical follow-up from a subgroup of patients who consented to subsequent blood analysis (n=10). The clinical follow-up consisted of a complete clinical evaluation by a urologist, including radiologic studies to evaluate RCC relapse. Healthy controls were sampled only at the beginning of the study (n=10). Furthermore, after completing histopathological analysis, 2 g of tumor tissue was sampled from the macroscopically defined tumor area in each nephrectomized kidney. The histopathological analysis consisted of RCC subtype diagnosis, pathological tumor staging (pTNM) according to the American Joint Committee on Cancer guidelines (15), evaluation of tumor grade according to the International Society of Urological Pathology (ISUP) grading system (16), presence of tumor necrosis and identification of sarcomatoid or rhabdoid differentiation.

Immunohistochemistry. All studied samples underwent a comprehensive assessment for multifocality, necrosis and sarcomatoid features. Representative sections of formalin-fixed paraffin-embedded tissues were used for further analyses. Briefly, the tissues were fixed with 10% neutral-buffered formalin for 24 h at room temperature. After fixation, tissues were embedded in paraffin and sliced to obtain 4-μm-thick sections. Subsequently, the tissues were rehydrated through a series of alcohol solutions, from absolute to 70% ethanol, finishing with distilled water. Since standard formalin-fixed, paraffin-embedded sections do not require permeabilization, this step was not performed. Immunostaining was performed using the OptiView DAB IHC Detection Kit (cat. no. 760-700; Roche Tissue Diagnostics; Roche Diagnostics, Ltd.) and the BenchMark ULTRA stainer module (cat. no. 05342716001; Roche Tissue Diagnostics; Roche Diagnostics, Ltd.). The OptiView detection kit includes reagents for peroxidase inhibition, biotin-free hapten-coupled secondary antibody and horseradish peroxidase multimer coupled tertiary antibodies. Chromogenic reaction was performed with the 3,3'-diaminobenzidine tetrahydrochloride (DAB) chromogen. Antigen retrieval was performed using Discovery CC1 solution (cat. no. 950-500; Roche Diagnostics, Ltd.) for 64 min at 100˚C. The primary antibodies used were mouse monoclonal anti-CTLA-4 (cat. no. BSB 2880; clone BSB-88; Bio SB, Inc.), rabbit monoclonal anti-PD-L1 (cat. no. 790-4905; clone SP263; Roche Tissue Diagnostics; Roche Diagnostics, Ltd.) and rabbit monoclonal anti-CD3 (cat. no. 790-4341; clone 2GV6; Roche Tissue Diagnostics; Roche Diagnostics, Ltd.) at a dilution of 1:50 for 32 min at 37˚C. The secondary reaction was performed using the OptiView DAB Detection Kit for an additional 12 min at 37˚C. All staining procedures were performed according to the manufacturer's protocol to ensure consistency and reliability. Clinical analyses of all samples were performed by three clinical pathologists using a brightfield optical microscope (Olympus CX31; Olympus Corporation).

The DP200 slide scanner (cat. no. 08303916001; Roche Tissue Diagnostics; Roche Diagnostics, Ltd.) was used for whole-slide scanning. Subsequently, a set of 8-10 randomly selected images (magnification, x40) were further analyzed using the QuPath software for Windows (version 0.5.1) (17). Digital analyses were performed by a trained non-pathologist (Fig. S1). The percentage of positive cells was calculated using the following formula: Percentage of positive cells=[number of positive cells/(number of positive cells + number of negative cells)] x100.

Flow cytometry. Cytometric analyses of blood samples were performed on the day of nephrectomy (n=7-12) and after a 12-month clinical follow-up (n=10). Some of the blood samples were lost during the procedure due to a technical error, and only samples deemed acceptable after quality control were included, defined as properly anticoagulated blood and a viability >50% based on trypan blue exclusion (n=7-12). For tissue analysis (n=18), the tumor was mechanically and enzymatically digested in DMEM supplemented with 5% FBS (cat. no. F2442; Sigma-Aldrich; Merck KGaA). The enzyme cocktail contained collagenase (cat. no. C9891; MilliporeSigma), hyaluronidase (cat. no. H3506; MilliporeSigma), DNase (cat. no. 10104159001; Roche Diagnostics, Ltd.) and trypsin (cat. no. 15090-046; Gibco; Thermo Fisher Scientific, Inc.) with EGTA (cat. no. E3889; MilliporeSigma). Furthermore, the tissues were incubated with the protease dispase (cat. no. 17105041; Gibco; Thermo Fisher Scientific, Inc.) and BD FACS™ Lysing Solution (cat.

Table I. Clinical characteristics of the participants.

Variable	Control (n=10)	Patients (n=20)	P-value
Sex, n (%)			0.139[a]
Male	4 (40)	14 (70)	
Female	6 (60)	6 (30)	
Age, years ± SD	60.8±6.0	59.4±8.0	0.610[b]
Tumor size, cm ± SD	-	8.2±3.9	-
Necrosis <50%, n (%)	-	18 (90)	-
Nuclear grade, n (%)			
G2	-	6 (30)	-
G3	-	9 (45)	-
G4	-	5 (25)	-
T stage, n (%)			
T1	-	6 (30)	-
T2	-	2 (10)	-
T3	-	10 (50)	-
T4	-	2 (10)	-

[a]Fisher's exact test. [b]Unpaired Student's t-test.

no. 349202; BD Biosciences) for 10 min at room temperature. After eliminating the aggregates with a 70 μm cell strainer (cat. no. 352350; Falcon; Corning Life Sciences), 1x10^6 cells were stained. Complete blood samples (50 μl) were stained, followed by erythrocyte lysis for 20 min. The antibody cocktail for lymphocytes (CD3$^+$, CD4$^+$ and CD8$^+$ lymphocytes) contained FITC mouse anti-human CD8 (20 μl/sample; cat. no. 555366; clone RPA-T8), PE mouse anti-human CD279 (PD-1; 20 μl/sample; cat. no 557946; clone MIH4), BV605 mouse anti-human CD4 (5 μl/sample; cat. no. 562658; clone RPA-T4), APC-Cy™7 mouse anti-human CD3 (5 μl/sample; cat. no. 557832; clone SK7), Alexa Fluor® 647 mouse anti-human CD366 (TIM-3; 5 μl/sample; cat. no. 565558; clone 7D3), PE-CF594 mouse anti-human CD223 (LAG-3; 5 μl/sample; cat. no. 565718; clone T47-530) and BV421 mouse anti-human CD152 (CTLA-4; 5 μl/sample; cat. no. 562743; clone BNI3). The antibody cocktail for myeloid cells (granulocytes and monocytes) contained Alexa Fluor® 488 mouse anti-human CD14 (5 μl/sample; cat. no. 557700; clone M5E2), BV421 mouse anti-human CD274 (PD-L1; 5 μl/sample; cat. no. 563738; clone MIH1), PE mouse anti-human CD45 (5 μl/sample; cat. no. 561866; clone HI30) and 7-AAD viability solution (5 μl/sample; cat. no. 559925). All antibodies were acquired from BD Biosciences.

For each sample, 1x10^5 events were acquired using an LSRFortessa flow cytometer (Becton, Dickinson and Company) and analyzed with DIVA version 8.0 for Windows (BD Biosciences). The percentages of CD4$^+$ and CD8$^+$ cells were quantified relative to CD3$^+$ cells. Similarly, the percentages of lymphocytes (CD14$^-$SSC^{lo}), monocytes (CD14$^+$SSC^{lo}) and granulocytes (CD14$^-$SSC^{hi}) were quantified relative to CD45$^+$ cells (Fig. S2). PD-1, LAG-3, TIM-3, CTLA-4 and PD-L1 fluorescence was analyzed as the mean fluorescence intensity (Fig. S3).

Statistical analysis. After confirming the parametric distribution of the data, an unpaired Student's t-test or one-way ANOVA followed by Bonferroni's multiple comparisons test was used for two- and three-group comparisons, respectively. Fisher's exact test was used to compare the sex proportions between patients and healthy controls and between tumor grade categories (Grade 2 vs. Grade >2). Statistical analyses were performed using GraphPad Prism (version 5.0; Dotmatics) for Windows and Microsoft Excel. P<0.05 was considered to indicate a statistically significant difference.

Results

Clinical description of the participants. Both groups of participants had similar ages and comorbidities, such as high blood pressure, type 2 diabetes and obesity. The mean age ± SD of the participants was 59.4±8 years in the patient group and 60.8±6 years in the healthy control group. A total of 10 patients were classified as T3 on the pTNM staging system and 14 patients had an ISUP nuclear grade ≥3. The average tumor size was 8.2±3.9 cm (Table I).

Immunohistochemistry reveals increased infiltration of the tumor tissue by CD3$^+$ lymphocytes. Serial sections from RCC tissue were stained for CD3, CTLA-4 and PD-L1 for immunohistochemical analysis. Positivity was evaluated by both clinical pathologists and digital analysis of micrographs using QuPath software (see Materials and methods; Fig. S1). Of all the tumor samples, >80% were positive for CD3 (Fig. 1A). By contrast, CTLA-4 (Fig. 1B) and PD-L1 (Fig. 1C) were positive in only 50 and 25% of the samples, respectively. These findings demonstrate that ccRCC tissue is highly infiltrated with lymphocytes and has low expression of the exhaustion markers CTLA-4 and PD-L1.

CD8$^+$ lymphocytes and monocytes dominates the tissue cellularity among infiltrating leukocytes. In addition to immunohistochemistry, flow cytometric analysis of tumor tissue and peripheral blood was performed to evaluate the changes in leukocyte dynamics (Figs. 2 and S2). The tumor tissue exhibited decreased infiltration of granulocytes and increased infiltration of monocytes and lymphocytes compared with the leukocyte percentages in the blood (Figs. 2A and S2A, C and E). Among the lymphocyte subpopulations, CD8$^+$ lymphocytes were the dominant subpopulation in the tumor tissue; notably, the percentage CD4$^+$ lymphocytes was markedly lower (Figs. 2B and S2B, D and F). There was a trend for increased percentages of granulocytes and CD4$^+$ and CD8$^+$ lymphocytes in blood from patients compared with blood from healthy controls; however, the differences were not statistically significant.

Tumor-infiltrating leukocytes demonstrate decreased expression levels of the markers LAG-3, TIM-3, CTLA-4 and PD-L1. After assessing leukocyte dynamics, the expression levels of several receptors associated with lymphocyte exhaustion were evaluated, a principal mechanism involved in antitumor immunity. Using flow cytometry, the expression levels of PD-1, LAG-3, TIM-3 and CTLA-4 in lymphocytes, and PD-L1 receptors in granulocytes and monocytes were

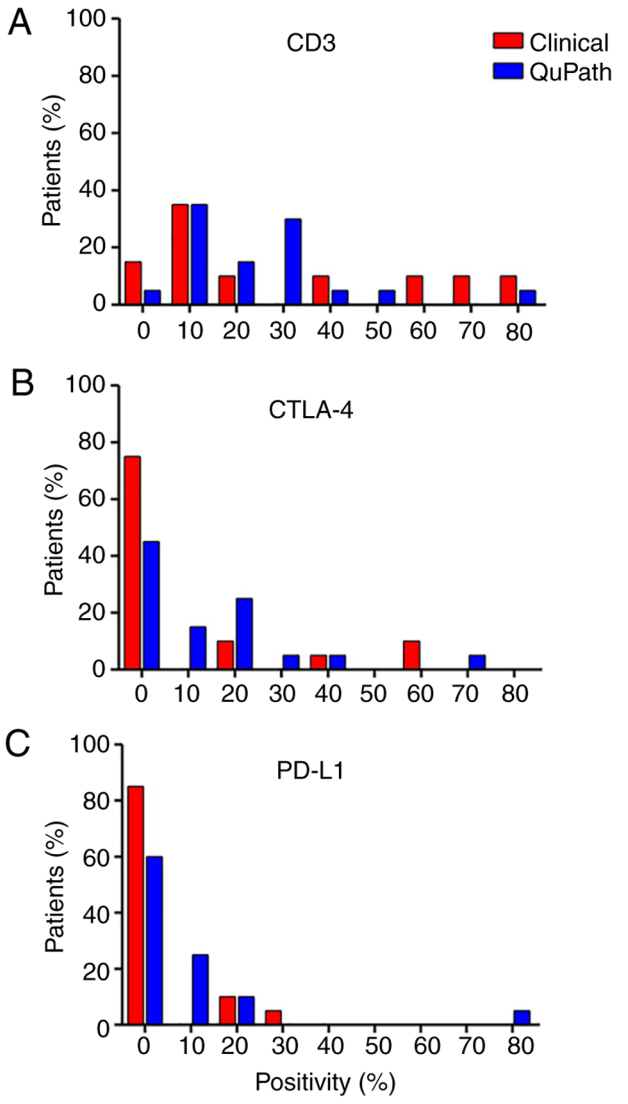


Figure 1. ccRCC tumors are highly positive for CD3 but mostly negative for CTLA and PD-L1. The tumor tissue from 20 patients was analyzed for (A) CD3, (B) CTLA-4 and (C) PD-L1 expression using immunohistochemistry. The percentage of positive tissue was quantified using two approaches: Clinical analysis by a group of pathologists and digital analysis from scanned slides using QuPath software. ccRCC, clear cell renal cell carcinoma; PD-L1, programmed death-ligand 1; PD-1, programmed cell death protein-1; LAG-3, lymphocyte activation gene-3; TIM-3, T-cell immunoglobulin and mucin domain-containing protein-3; CTLA-4, cytotoxic T lymphocyte-associated protein-4.

evaluated (Figs. 3 and S3). There was no change in PD-1 expression (Figs. 3A-C and S3A) but decreased expression levels of LAG-3 (Figs. 3D-F and S3B), TIM-3 (Figs. 3H-I and S3C) and CTLA-4 (Figs. 3J-L and S3D) among tumor-infiltrating lymphocytes were observed compared with blood samples. In addition, decreased PD-L1 expression levels were reported in granulocytes (Fig. 3M) and monocytes (Figs. 3N and S3E) that infiltrated the tumor tissue compared with the blood. Only two markers indicated expression differences between the patient and healthy control blood samples. The patients had increased TIM-3 levels (Fig. 3G) and decreased PD-L1 levels (Fig. 3N) in lymphocytes and monocytes, respectively. Collectively, the present study results demonstrate decreased expression of several exhaustion-associated markers within tumor-infiltrating lymphocytes, with the notable exception of PD-1.

Patient stratification according to nuclear grade indicates no differences in the expression of exhaustion markers. To assess the clinical significance of quantifying the exhaustion-associated markers, the differential expression of these markers was evaluated according to the tumor nuclear grade (Table II). No overall differences in marker expression associated with nuclear grade were reported, except for CD3 positivity based on immunohistochemistry. Furthermore, the temporal changes in blood expression levels of the tested markers were compared 12 months after therapeutic nephrectomy (Table III). The only change observed was an increase in CTLA-4 expression levels in blood lymphocytes at 12 months compared with basal levels. Collectively, ccRCC tissue exhibited increased proportions of infiltrated $CD3^+$ lymphocytes and monocytes compared with the proportions in the blood (Figs. 1 and 2). Infiltrated leukocytes showed decreased expression levels of the exhaustion markers LAG-3, TIM-3, CTLA-4 and PD-L1, but not PD-1 (Fig. 3). Furthermore, the variables did not change after stratifying the patients according to nuclear grade and between baseline and clinical follow-up (Tables II and III).

Discussion

RCC primarily affects patients aged 60 to 70 years old (2). Among its variants, up to 80% of the diagnoses are associated with ccRCC, a severe disease characterized by intrinsic aggressiveness, chemoresistance and poor prognosis (3,6). In the early stages, ccRCC may be cured through nephrectomy; however, advanced disease often requires systemic and combined therapies such as immunotherapy and systemic targeted therapy (5). These treatments present challenges, particularly due to the lack of validated tools for selecting patients based on their likelihood of clinical response and the risk of adverse events (13,14). The role of infiltrating leukocytes in prognosis and response to treatment is not completely understood and depends on characteristics such as the cell phenotype, tumor infiltration and the cell exhaustion status (7). For example, the increased infiltration of $CD8^+$ and $CD68^+$ cells and decreased infiltration of $CD4^+$ cells predict a positive response to ICI treatment (18). However, in general, tumor-infiltrating lymphocytes are commonly associated with poor prognosis (19). Particularly in RCC, highly infiltrated tumors (also called hot tumors) are associated with poor prognosis (20). Among exhaustion markers, the increased expression of PD-L1 is found in ~6% of patients with RCC and is commonly associated with poor outcomes (21). The relationship between systemic inflammation and RCC prognosis has also been investigated, revealing a negative association between these variables (22). For these reasons, the expression levels of exhaustion receptors should be interpreted with caution because, while increased levels of PD-L1 are commonly associated with poor overall prognosis, the increased availability of these ligands could be predictive of the success of ICI treatments (23). There is a lack of information regarding the temporal expression of molecular immunotherapy targets among tumors and tumor stages, including kidney tumors.

Table II. Analysis of leukocyte markers according to tumor grade G2-G4.

Variable	G2 (n=6)	G3 (n=9)	G4 (n=5)	P-value[a]
Sex, n (%)				0.354
Male	5 (83)	5 (55)	3 (60)	
Female	1 (17)	4 (45)	2 (40)	
Age, years ± SD	61.5±8.6	59.7±8.9	60.2±7.7	0.919
Tumor size, cm ± SD	7.2±3.2	7.8±5.1	8.6±2.4	0.851
Necrosis, % ± SD	16.7±17.2	15.5±19.8	22.5±14.7	0.744
Positive tissue on immunohistochemistry, % ± SD				
CD3	13.4±7.6	19.8±14.6	39.6±22.0	0.030
CD3 (clinical)	14.3±22.6	25.6±30.7	54.0±24.1	0.071
CTLA-4	14.9±25.7	13.1±14.7	9.4±10.0	0.876
CTLA-4 (clinical)	17.0±26.3	8.6±19.9	4.2±8.8	0.566
PD-L1	16.6±31.0	6.8±5.8	0.6±0.5	0.322
PD-L1 (clinical)	0.5±0.5	5.8±11.2	4.8±8.5	0.514
Flow cytometry of blood samples, MFI ± SD				
PD-L1 granulocytes	6,975±5,007	6,165±2,272	8,873±4,598	0.669
PD-L1 monocytes	5,486±3,618	9,543±5,709	9,414±2,200	0.356
PD-1 CD3	475±158	925±577	2,357±2,451	0.134
LAG-3 CD3	662±238	1,000±530	3,093±3,319	0.122
TIM-3 CD3	552±288	775±336	1,309±840	0.130
CTLA-4 CD3	692±226	1,166±724	4,285±5,624	0.181
Flow cytometry of tumor samples, MFI ± SD				
PD-L1 granulocytes	6,797±6,332	6,031±7,207	2,207±1,010	0.588
PD-L1 monocytes	3,032±1,059	7,944±3,871	29451±48,419	0.162
PD-1 CD3	2,473±792	2,248±1,399	3,128±2,616	0.729
LAG-3 CD3	1,301±294	1,488±930	1,452±768	0.927
TIM-3 CD3	502±258	731±501	1,139±1,015	0.395
CTLA-4 CD3	444±227	801±876	1,052±816	0.524

[a]All variables were compared with one-way ANOVA, except for sex, which was analyzed with the Fisher's exact test (G2 vs. G>2). PD-L1, programmed death-ligand 1; PD-1, programmed cell death protein-1; LAG-3, lymphocyte activation gene-3; TIM-3, T-cell immunoglobulin and mucin domain-containing protein- 3; CTLA-4, cytotoxic T lymphocyte-associated protein-4; MFI, mean fluorescence intensity.

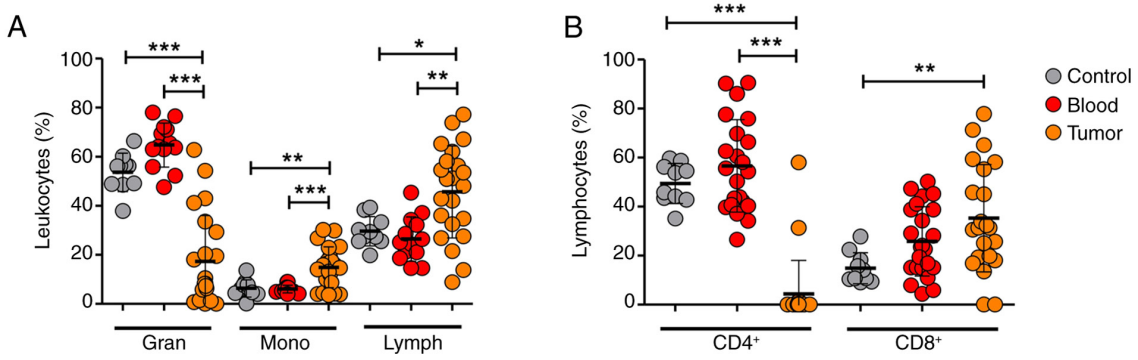


Figure 2. In tumor tissue, cellularity is dominated by CD8+ lymphocytes and monocytes. The percentage of leukocytes (A) and lymphocytes (B) were evaluated in the blood and tumors using flow cytometry. For blood, there were no differences between healthy controls (control) and patients (blood). In tumors, there was an increased percentage of monocytes and CD8+ lymphocytes, a decreased percentage of granulocytes and almost no CD4+ lymphocytes, compared with blood samples. Mean ± SD n=10 (control); n=14-21 (blood and tumor). One-way ANOVA with Bonferroni's post hoc test. *P<0.05; **P<0.01; ***P<0.001. ccRCC, clear cell renal cell carcinoma; Gran, granulocytes; Mono, monocytes; Lymph, lymphocytes.

To address this issue, the present study aimed to characterize the expression of five common immunotherapy targets, PD-1, PD-L1, LAG-3, TIM-3 and CTLA-4, in tissue and blood samples obtained from a cohort of 20 patients with localized

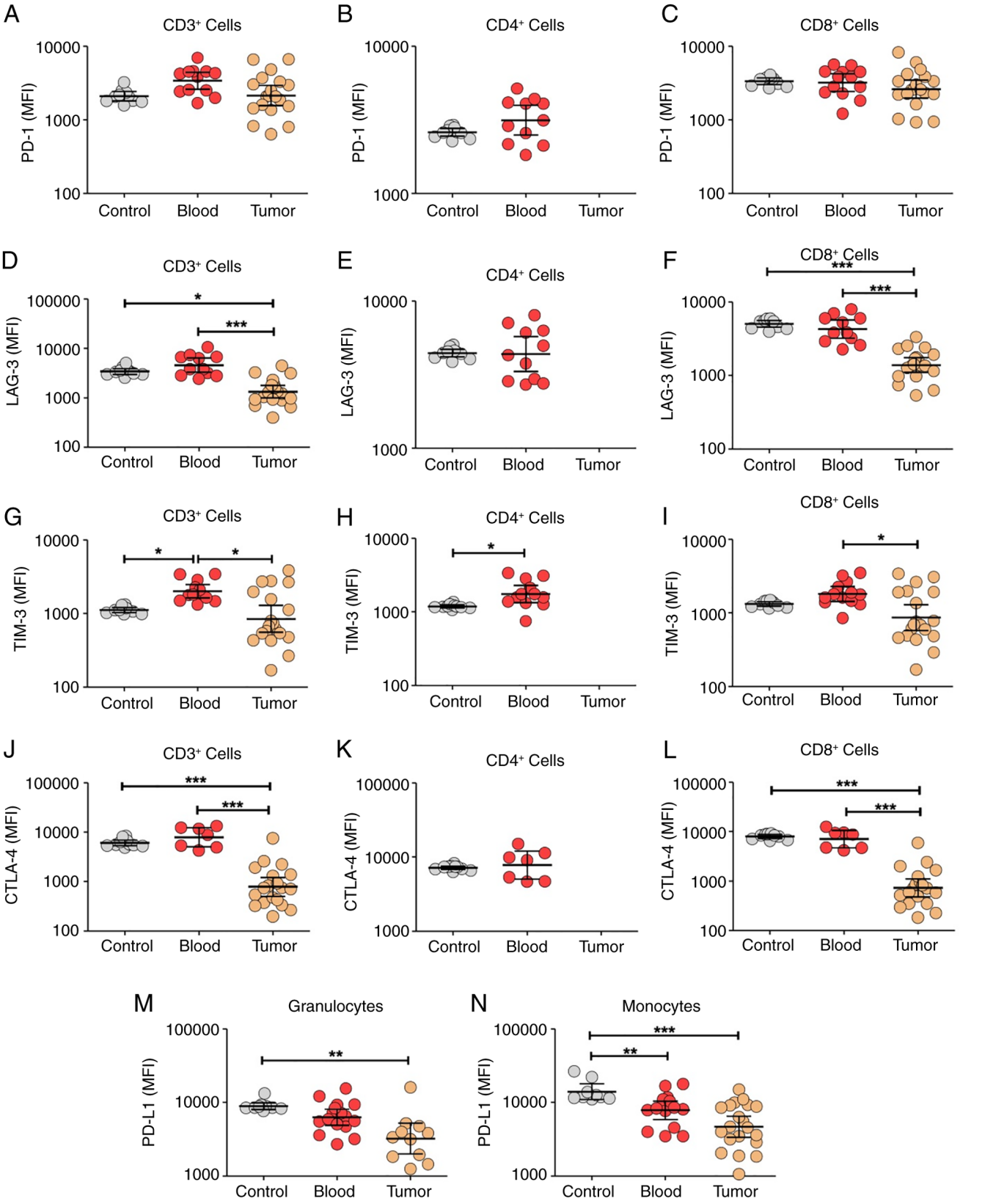


Figure 3. Compared with circulating leukocytes, tumor-infiltrating leukocytes exhibit decreased expression of the exhaustion receptors LAG-3, TIM-3, CTLA-4 and PD-L1 based on flow cytometry. All receptors were evaluated in blood leukocytes from healthy controls (control), blood leukocytes from patients (blood) and tumor-infiltrating leukocytes (tumor). PD-1 was evaluated in (A) $CD3^+$, (B) $CD4^+$ and (C) $CD8^+$ lymphocytes. LAG-3 was evaluated in (D) $CD3^+$, (E) $CD4^+$ and (F) $CD8^+$ lymphocytes. TIM-3 was evaluated in (G) $CD3^+$, (H) $CD4^+$ and (I) $CD8^+$ lymphocytes. CTLA-4 was evaluated in (J) $CD3^+$, (K) $CD4^+$ and (L) $CD8^+$ lymphocytes. PD-L1 was evaluated in (M) granulocytes and (N) monocytes. The tumor-infiltrating leukocytes exhibited decreased expression levels of LAG-3, TIM-3, CTLA-4 and PD-L1 compared with blood leukocytes, but no changes were observed in PD-1 expression. Data are expressed as MFI ± SD. Control group, n=10; blood group, n=7-12; tumor group, n=18. Data were analyzed using one-way ANOVA with Bonferroni's post hoc test (except panels B, E, H and K, which were analyzed using an unpaired Student's t-test). $^*P<0.05$; $^{**}P<0.01$; $^{***}P<0.001$. PD-L1, programmed death-ligand 1; PD-1, programmed cell death protein-1; LAG-3, lymphocyte activation gene-3; TIM-3, T-cell immunoglobulin and mucin domain-containing protein-3; CTLA-4, cytotoxic T lymphocyte-associated protein-4; MFI, mean fluorescence intensity.

Table III. Changes in leukocyte markers at 12 months follow-up using flow cytometry.

Variable	Basal (n=20)	12 months (n=10)	P-value[a]
Granulocytes, % ± SD	34.2±32.9	45.4±21.4	0.320
Monocytes, % ± SD	12.2±11.0	7.4±2.3	0.166
Lymphocytes, % ± SD	48.3±25.7	42.0±21.4	0.497
$CD4^+$, % ± SD	56.3±18.1	52.8±15.1	0.604
$CD8^+$, % ± SD	24.6±13.8	18.1±9.2	0.197
PD-L1, MFI ± SD			
Monocytes	6,135±3,916	6,807±4,716	0.674
Granulocytes	15,867±27,880	4,951±3,556	0.232
PD-1, MFI ± SD			
$CD3^+$	2,320±1,821	3,160±1,967	0.260
$CD4^+$	1,973±1,534	2,993±1,768	0.118
$CD8^+$	2,570±1,499	3,041±1,779	0.457
LAG-3, MFI ± SD			
$CD3^+$	3,043±2,802	1,771±1,208	0.185
$CD4^+$	2,840±2,321	1,826±1,192	0.209
$CD8^+$	2,805±2,272	1,464±968	0.088
TIM-3, MFI ± SD			
$CD3^+$	1,358±805	1,263±817	0.766
$CD4^+$	1,301±772	1,210±746	0.762
$CD8^+$	1,317±744	1,193±786	0.680
CTLA-4, MFI ± SD			
$CD3^+$	3,672±4,437	8,416±6,330	0.026
$CD4^+$	3,902±4,297	8,539±6,102	0.024
$CD8^+$	3,012±4,058	6,743±5,130	0.041

[a]All variables were analyzed with an unpaired Student's t-test. PD-L1, programmed death-ligand 1; PD-1, programmed cell death protein-1; LAG-3, lymphocyte activation gene-3; TIM-3, T-cell immunoglobulin and mucin domain-containing protein- 3; CTLA-4, cytotoxic T lymphocyte-associated protein-4; MFI, mean fluorescence intensity.

ccRCC, an early stage of the disease. According to the literature, the 5-year cancer-specific survival rates for stage I, II, III and IV patients are 97.4, 89.9, 77.9 and 26.7%, respectively, and nephrectomy improves the condition-specific survival, mostly in advanced tumors (stages III and IV) (24).

The immunohistochemistry results of the present study aligned with those of previous reports that characterize ccRCC as a highly immunogenic tumor (25). The tumor tissue indicated increased expression levels of CD3, but moderate-to-absent expression of CTLA-4 and PD-L1. In the majority of cancer types, elevated CD3 expression is generally associated with a favorable prognosis and response to systemic immunotherapy (26-29); however, previous studies suggest the opposite for ccRCC, where high infiltration of lymphocytes and increased expression of exhaustion markers have been associated with poor overall prognosis and unresponsiveness to immunotherapy (25,30,31). The present study assessed the immunohistochemistry data using two approaches: Clinical analysis by pathologists and digital analysis using the QuPath software. From an objective point of view, digital analysis would overcome the possibility of subjective or biased analysis, although it is more complex and usually restricted to research settings.

Following immunohistochemistry, the present study adopted flow cytometry to evaluate the expression of biomarkers in the blood and tissue samples. The integration of immunohistochemistry and flow cytometry followed the rationale that combined methods would enable a broader and more accurate assessment of immune exhaustion compared with each method alone. Flow cytometry was selected as a complementary technique to immunohistochemistry due to its capacity for high-dimensional, single-cell analysis, which allows for the precise quantification of immune subsets and co-expression of exhaustion markers. In the flow cytometry analysis, the present study evaluated the expression of a set of biomarkers commonly associated with lymphocyte exhaustion and targeted by therapeutic monoclonal antibodies in clinical oncology. The results demonstrated that the patients had a distinct pattern of infiltrating leukocytes, predominantly cytotoxic lymphocytes and monocytes. Evaluation of the tumor tissue indicated the absence of $CD4^+$ lymphocytes and a relative increase in $CD3^+CD4^-CD8^-$ cells (data not shown). A decrease in the number of infiltrating $CD4^+$ cells has been associated with poor prognosis in patients with sarcoma and cervical carcinoma (32,33). The relative increase in $CD3^+CD4^-CD8^-$ cells and the abundance of lipids within the tumor core suggest

the presence of natural killer T lymphocytes because such cells have intrinsic capabilities to recognize lipidic antigens (34,35). Furthermore, ccRCC has been associated with the presence of circulating double-positive lymphocytes ($CD4^+CD8^+$) and dysfunctional lymphocytes in *ex vivo* assays (36-38). Other previous studies have also proposed the use of the neutrophil-to-lymphocyte ratio (39) and C-reactive protein serum levels (40,41) as potential cost-effective biomarkers for the prediction of immunotherapy response in advanced ccRCC.

After assessing lymphocyte kinetics, the present study investigated the expression of exhaustion-associated markers using flow cytometry. Among circulating leukocytes, patients had increased TIM-3 expression levels in blood lymphocytes and decreased PD-L1 expression levels in blood monocytes compared with that of the control group. In tumors, unchanged expression levels of PD-1 and decreased expression levels of LAG-3, TIM-3, CTLA-4 and PD-L1 were reported compared with those in the blood samples. Similarly, PD-L1 expression levels decreased among infiltrating monocytes and granulocytes. These results suggest that mild leukocyte dysfunction is present in the localized stage of ccRCC, but there is uncertainty about the implications of these findings in the later response to ICIs in advanced disease, mostly because the immune exhaustion phenomenon is highly dynamic. It is important to highlight that immune exhaustion is a complex mechanism involving multiple receptors and cell phenotypes (42-44). For example, exhausted $CD8^+$ cells promote tumor progression, but exhausted T regulatory (Treg) lymphocytes inhibit tumor progression (45). Treg lymphocytes mediate immunosuppression in T cells and dendritic cells by producing the regulatory cytokines interleukin-10 and transforming growth factor-β (45). Therefore, detailed and comprehensive studies addressing multiple markers are warranted to predict immunotherapy responses. Increased expression levels of TIM-3 in lymphocytes and decreased expression levels of PD-L1 in monocytes have been associated with worse outcomes in patients diagnosed with RCC (46,47).

To assess the clinical significance of biomarker expression in patients with RCC, patients were stratified based on nuclear grade, due to the well-established inverse association between nuclear grade and clinical outcomes (31,48). The present study results did not indicate changes in tissue leukocyte dynamics and biomarker expression compared with nuclear grade, except for an increased percentage of CD3 positivity in grade 4 tumors (Table II). In the same context, when evaluating the changes in blood biomarker expression after 12 months of clinical follow-up, the present study demonstrated that most markers were stable over time, with the notable exception of CTLA-4 (Table III). These results suggest that the expression of exhaustion biomarkers in localized disease was not associated with the nuclear grade staging and did not demonstrate variation in the short-term follow-up of 12-months.

The overall results of the present study suggest that localized ccRCC shows decreased expression levels of the exhaustion receptors LAG-3, TIM-3, CTLA-4 and PD-L1, implying a lack of biological support for an immune exhaustion state in this stage of the disease. In the future, it will be necessary to analyze an expanded set of markers (OX40, 4-1BB, TOX and interleukin-10) and cell phenotypes (T regulatory lymphocytes, myeloid-derived suppressor cells and tumor-associated macrophages) in localized and metastatic disease to shed light on the progressive expression of such biomarkers in RCC.

The present study had several limitations, including the small number of participants, which followed the exclusion of samples with insufficient cell counts to ensure reliable results and the short-term follow-up of patients, which complicates the clinical significance of the findings. In addition, tissue samples were compared with blood samples because obtaining healthy renal tissue is challenging due to ethical and practical reasons. However, the findings remain notable due to the clinical nature of the present study, the combined use of immunohistochemistry and flow cytometry, simultaneous analysis of tumor and blood samples and homogeneous inclusion of patients with localized disease. In the future, a prospective study is warranted to assess an extended panel of biomarkers as prognostic and predictive tools to guide the use of immunotherapy in patients with RCC.

ccRCC is highly infiltrated by lymphocytes and patients demonstrate decreased expression levels of the exhaustion biomarkers LAG-3, TIM-3, CTLA-4 and PD-L1 within infiltrating tumor leukocytes compared with circulating leukocytes. These biomarkers remain stable in the short term and are not associated with nuclear grade staging, which suggest they have limited use as a prognostic tool in localized ccRCC.

Acknowledgements

Not applicable.

Funding

The present study was supported by the National Science and Technology Council (CONACYT), México (grant no. 301133).

Availability of data and materials

The data generated in the present study may be found on Figshare at the following URL: https://figshare.com/articles/dataset/Flow_cytometry_data_for_tissue_leukocytes_in_a_cohort_of_20_patients_with_clear_cells_renal_cell_carcinoma/26888827/1.

Authors' contributions

RGGa, MMT, AGG and MCSC conceptualized and designed the present study. RGGa, MMT and NLL developed and devised the methodology. MMT and RGGu supervised the present study. RGGa, AGG, VMOJ and MAOM were involved in the clinical evaluation and follow-up of patients. MMT and RGGa acquired and analyzed the data for flow cytometry. JPFG, RGGa, RGGu and JHEJ were involved in the immunohistochemistry analysis. RGGa, MAOM and MMT wrote the first draft. MMT, MCSC, VMOJ and NLL revised and corrected the manuscript. RGGa and MMT confirm the authenticity of all the raw data. All authors read and approved the final version of the manuscript.

Ethics approval and consent to participate

The present study was approved by the institutional ethics committee (approval no. IN23-00002). All patients provided written informed consent before enrollment in the present study.

Patient consent for publication

Not applicable.

Competing interests

The authors declare that they have no competing interests.

References

1. Padala SA, Barsouk A, Thandra KC, Saginala K, Mohammed A, Vakiti A, Rawla P and Barsouk A: Epidemiology of renal cell carcinoma. World J Oncol 11: 79-87, 2020.
2. Rose TL and Kim WY: Renal cell carcinoma: A review. JAMA 332: 1001-1010, 2024.
3. Di S, Gong M, Lv J, Yang Q, Sun Y, Tian Y, Qian C, Chen W, Zhou W, Dong K, *et al*: Glycolysis-related biomarker TCIRG1 participates in the regulation of renal cell carcinoma progression and tumor immune microenvironment by affecting aerobic glycolysis and AKT/mTOR signaling pathway. Cancer Cell Int 23: 186, 2023.
4. Ma G, Wang Z, Liu J, Fu S, Zhang L, Zheng D, Shang P and Yue Z: Quantitative proteomic analysis reveals sophisticated metabolic alteration and identifies FMNL1 as a prognostic marker in clear cell renal cell carcinoma. J Cancer 12: 6563-6575, 2021.
5. Scosyrev E, Messing EM, Sylvester R and Van Poppel H: exploratory subgroup analyses of renal function and overall survival in European organization for research and treatment of cancer randomized trial of nephron-sparing surgery versus radical nephrectomy. Eur Urol Focus 3: 599-605, 2017.
6. Bahadoram S, Davoodi M, Hassanzadeh S, Bahadoram M, Barahman M and Mafakher L: Renal cell carcinoma: An overview of the epidemiology, diagnosis, and treatment. G Ital Nefrol 39: 2022-vol3, 2022.
7. González-Garza R, Gutiérrez-González A, Salinas-Carmona M and Mejía-Torres M: Biomarkers for evaluating the clinical response to immune checkpoint inhibitors in renal cell carcinoma (Review). Oncol Rep 52: 164, 2024.
8. Jiang X, Liu G, Li Y and Pan Y: Immune checkpoint: The novel target for antitumor therapy. Genes Dis 8: 25-37, 2021.
9. Motzer RJ, Alyasova A, Ye D, Karpenko A, Li H, Alekseev B, Xie L, Kurteva G, Kowalyszyn R, Karyakin O, *et al*: Phase II trial of second-line everolimus in patients with metastatic renal cell carcinoma (RECORD-4). Ann Oncol 27: 441-448, 2016.
10. Motzer RJ, Tannir NM, McDermott DF, Frontera OA, Melichar B, Choueiri TK, Plimack ER, Barthélémy P, Porta C, George S, *et al*: Nivolumab plus ipilimumab versus sunitinib in advanced renal-cell carcinoma. N Engl J Med 378: 1277-1290, 2018.
11. Motzer RJ, Penkov K, Haanen J, Rini B, Albiges L, Campbell MT, Venugopal B, Kollmannsberger C, Negrier S, Uemura M, *et al*: Avelumab plus axitinib versus sunitinib for advanced renal-cell carcinoma. N Engl J Med 380: 1103-1115, 2019.
12. Rini BI, Powles T, Atkins MB, Escudier B, McDermott DF, Suarez C, Bracarda S, Stadler WM, Donskov F, Lee JL, *et al*: Atezolizumab plus bevacizumab versus sunitinib in patients with previously untreated metastatic renal cell carcinoma (IMmotion151): A multicentre, open-label, phase 3, randomised controlled trial. Lancet 393: 2404-2415, 2019.
13. Wang DY, Salem JE, Cohen JV, Chandra S, Menzer C, Ye F, Zhao S, Das S, Beckermann KE, Ha L, *et al*: Fatal toxic effects associated with immune checkpoint inhibitors. JAMA Oncol 4: 1721-1728, 2018.
14. Saliby RM, Saad E, Kashima S, Schoenfeld DA and Braun DA: Update on biomarkers in renal cell carcinoma. American Society of Clinical Oncology Educational Book 44: 2, 2024.
15. Amin MB, American Joint Committee on Cancer, and American Cancer Society: AJCC cancer staging manual. Eight edition/editor-in-chief, Mahul B. Amin, MD, FCAP; editors, Stephen B. Edge, MD, FACS [and 16 others]; Donna M. Gress, RHIT, CTR-Technical editor ; Laura R. Meyer, CAPM-Managing editor. American Joint Committee on Cancer, Springer, Chicago IL, 2017.
16. Organisation mondiale de la santé and Centre international de recherche sur le cancer: Urinary and male genital tumours. 5th ed. International agency for research on cancer, Lyon, 2022.
17. Bankhead P, Loughrey MB, Fernández JA, Dombrowski Y, McArt DG, Dunne PD, McQuaid S, Gray RT, Murray LJ, Coleman HG, *et al*: QuPath: Open source software for digital pathology image analysis. Sci Rep 7: 16878, 2017.
18. Kazama A, Bilim V, Tasaki M, Anraku T, Kuroki H, Shirono Y, Murata M, Hiruma K and Tomita Y: Tumor-infiltrating immune cell status predicts successful response to immune checkpoint inhibitors in renal cell carcinoma. Sci Rep 12: 20386, 2022.
19. Wu C, Cui Y, Liu J, Ma L, Xiong Y, Gong Y, Zhao Y, Zhang X, Chen S, He Q, *et al*: Noninvasive evaluation of tumor immune microenvironment in patients with clear cell renal cell carcinoma using metabolic parameter from preoperative 2-[^{18}F]FDG PET/CT. Eur J Nucl Med Mol Imaging 48: 4054-4066, 2021.
20. Ohe C, Yoshida T, Ikeda J, Tsuzuki T, Ohashi R, Ohsugi H, Atsumi N, Yamaka R, Saito R, Yasukochi Y, *et al*: Histologic-based tumor-associated immune cells status in clear cell renal cell carcinoma correlates with gene signatures related to cancer immunity and clinical outcomes. Biomedicines 10: 323, 2022.
21. Möller K, Fraune C, Blessin NC, Lennartz M, Kluth M, Hube-Magg C, Lindhorst L, Dahlem R, Fisch M, Eichenauer T, *et al*: Tumor cell PD-L1 expression is a strong predictor of unfavorable prognosis in immune checkpoint therapy-naive clear cell renal cell cancer. Int Urol Nephrol 53: 2493-2503, 2021.
22. Ozbek E, Besiroglu H, Ozer K, Horsanali MO and Gorgel SN: Systemic immune inflammation index is a promising non-invasive marker for the prognosis of the patients with localized renal cell carcinoma. Int Urol Nephrol 52: 1455-1463, 2020.
23. Kawashima A, Kanazawa T, Kidani Y, Yoshida T, Hirata M, Nishida K, Nojima S, Yamamoto Y, Kato T, Hatano K, *et al*: Tumour grade significantly correlates with total dysfunction of tumour tissue-infiltrating lymphocytes in renal cell carcinoma. Sci Rep 10: 6220, 2020.
24. Cheaib JG, Patel HD, Johnson MH, Gorin MA, Haut ER, Canner JK, Allaf ME and Pierorazio PM: Stage-specific conditional survival in renal cell carcinoma after nephrectomy. Urol Oncol 38: 6.e1-6.e7, 2020.
25. Giraldo NA, Becht E, Vano Y, Petitprez F, Lacroix L, Validire P, Sanchez-Salas R, Ingels A, Oudard S, Moatti A, *et al*: Tumor-Infiltrating and peripheral blood T-cell immunophenotypes predict early relapse in localized clear cell renal cell carcinoma. Clin Cancer Res 23: 4416-4428, 2017.
26. Jung M, Lee JA, Yoo SY, Bae JM, Kang GH and Kim JH: Intratumoral spatial heterogeneity of tumor-infiltrating lymphocytes is a significant factor for precisely stratifying prognostic immune subgroups of microsatellite instability-high colorectal carcinomas. Mod Pathol 35: 2011-2022, 2022.
27. Mei Z, Liu Y, Liu C, Cui A, Liang Z, Wang G, Peng H, Cui L and Li C: Tumour-infiltrating inflammation and prognosis in colorectal cancer: Systematic review and meta-analysis. Br J Cancer 110: 1595-1605, 2014.
28. Tewari N, Zaitoun AM, Arora A, Madhusudan S, Ilyas M and Lobo DN: The presence of tumour-associated lymphocytes confers a good prognosis in pancreatic ductal adenocarcinoma: An immunohistochemical study of tissue microarrays. BMC Cancer 13: 436, 2013.
29. Rathore AS, Kumar S, Konwar R, Makker A, Negi MPS and Goel MM: CD3+, CD4+ & CD8+ tumour infiltrating lymphocytes (TILs) are predictors of favourable survival outcome in infiltrating ductal carcinoma of breast. Indian J Med Res 140: 361-369, 2014.
30. Kahlmeyer A, Stöhr CG, Hartmann A, Goebell PJ, Wullich B, Wach S, Taubert H and Erlmeier F: Expression of PD-1 and CTLA-4 are negative prognostic markers in renal cell carcinoma. J Clin Med 8: 743, 2019.
31. Kawakami F, Sircar K, Rodriguez-Canales J, Fellman BM, Urbauer DL, Tamboli P, Tannir NM, Jonasch E, Wistuba II, Wood CG and Karam JA: PD-L1 and tumor infiltrating lymphocytes status in patients with renal cell carcinoma and sarcomatoid dedifferentiation. Cancer 123: 4823-4831, 2017.
32. Bi Q, Liu Y, Yuan T, Wang H, Li B, Jiang Y, Mo X, Lei Y, Xiao Y, Dong S, *et al*: Predicted CD4+ T cell infiltration levels could indicate better overall survival in sarcoma patients. J Int Med Res 49: 0300060520981539, 2021.
33. Shah W, Yan X, Jing L, Zhou Y, Chen H and Wang Y: A reversed CD4/CD8 ratio of tumor-infiltrating lymphocytes and a high percentage of CD4+FOXP3+ regulatory T cells are significantly associated with clinical outcome in squamous cell carcinoma of the cervix. Cell Mol Immunol 8: 59-66, 2011.

34. Paul S, Chhatar S, Mishra A and Lal G: Natural killer T cell activation increases iNOS+CD206- M1 macrophage and controls the growth of solid tumor. J Immunother Cancer 7: 208, 2019.
35. Li J, Moresco P and Fearon DT: Intratumoral NKT cell accumulation promotes antitumor immunity in pancreatic cancer. Proc Natl Acad Sci USA 121: e2403917121, 2024.
36. Nishida K, Kawashima A, Kanazawa T, Kidani Y, Yoshida T, Hirata M, Yamamoto K, Yamamoto Y, Sawada M, Kato R, *et al*: Clinical importance of the expression of CD4+CD8+ T cells in renal cell carcinoma. Int Immunol 32: 347-357, 2020.
37. Menard LC, Fischer P, Kakrecha B, Linsley PS, Wambre E, Liu MC, Rust BJ, Lee D, Penhallow B, Orduno NM and Nadler SG: Renal cell carcinoma (RCC) tumors display large expansion of double positive (DP) CD4+CD8+ T cells with expression of exhaustion markers. Front Immunol 9: 2728, 2018.
38. Zelba H, Bedke J, Hennenlotter J, Mostböck S, Zettl M, Zichner T, Chandran A, Stenzl A, Rammensee HG and Gouttefangeas C: PD-1 and LAG-3 dominate checkpoint receptor-mediated T-cell inhibition in renal cell carcinoma. Cancer Immunol Res 7: 1891-1899, 2019.
39. Young M, Tapia JC, Szabados B, Jovaisaite A, Jackson-Spence F, Nally E and Powles T: NLR outperforms low hemoglobin and high platelet count as predictive and prognostic biomarker in metastatic renal cell carcinoma treated with immune checkpoint inhibitors. Clin Genitourin Cancer 22: 102072, 2024.
40. Ishihara H, Takagi T, Kondo T, Fukuda H, Tachibana H, Yoshida K, Iizuka J, Okumi M, Ishida H and Tanabe K: Predictive impact of an early change in serum C-reactive protein levels in nivolumab therapy for metastatic renal cell carcinoma. Urol Oncol 38: 526-532, 2020.
41. Noguchi G, Nakaigawa N, Umemoto S, Kobayashi K, Shibata Y, Tsutsumi S, Yasui M, Ohtake S, Suzuki T, Osaka K, *et al*: C-reactive protein at 1 month after treatment of nivolumab as a predictive marker of efficacy in advanced renal cell carcinoma. Cancer Chemother Pharmacol 86: 75-85, 2020.
42. Wei F, Zhong S, Ma Z, Kong H, Medvec A, Ahmed R, Freeman GJ, Krogsgaard M and Riley JL: Strength of PD-1 signaling differentially affects T-cell effector functions. Proc Natl Acad Sci USA 110: E2480-E2489, 2013.
43. Tsujikawa T, Kumar S, Borkar RN, Azimi V, Thibault G, Chang YH, Balter A, Kawashima R, Choe G, Sauer D, *et al*: Quantitative multiplex immunohistochemistry reveals myeloid-inflamed tumor-immune complexity associated with poor prognosis. Cell Rep 19: 203-217, 2017.
44. Pichler R, Siska PJ, Tymoszuk P, Martowicz A, Untergasser G, Mayr R, Weber F, Seeber A, Kocher F, Barth DA, *et al*: A chemokine network of T cell exhaustion and metabolic reprogramming in renal cell carcinoma. Front Immunol 14: 1095195, 2023.
45. Denize T, Jegede OA, Matar S, El Ahmar N, West DJ, Walton E, Bagheri AS, Savla V, Laimon YN, Gupta S, *et al*: PD-1 Expression on intratumoral regulatory T cells is associated with lack of benefit from anti-PD-1 therapy in metastatic clear-cell renal cell carcinoma patients. Clin Cancer Res 30: 803-813, 2024.
46. Cai C, Xu YF, Wu ZJ, Dong Q, Li MY, Olson JC, Rabinowitz YM, Wang LH and Sun Y: Tim-3 expression represents dysfunctional tumor infiltrating T cells in renal cell carcinoma. World J Urol 34: 561-567, 2016.
47. Yeong J, Zhao Z, Lim JCT, Li H, Thike AA, Koh VCY, Teh BT, Kanesvaran R, Toh CK, Tan PH and Khor LY: PD-L1 expression is an unfavourable prognostic indicator in Asian renal cell carcinomas. J Clin Pathol 73: 463-469, 2020.
48. Warren AY and Harrison D: WHO/ISUP classification, grading and pathological staging of renal cell carcinoma: Standards and controversies. World J Urol 36: 1913-1926, 2018.

Copyright © 2025 González-Garza et al. This work is licensed under a Creative Commons Attribution-NonCommercial-NoDerivatives 4.0 International (CC BY-NC-ND 4.0) License.